# POWER FLOW ANALYSIS OF ELECTROSTRICTIVE ACTUATORS DRIVEN BY SWITCHMODE AMPLIFIERS

Gregory A. Zvonar, Douglas K. Lindner
Bradley Department of Electrical and Computer Engineering
Virginia Tech
Blacksburg, VA 24061
Correspondence with D. Lindner @ (540) 231-4580, Fax: (540) 231-3362, Email: lindner@vt.edu

*Journal on Intelligent Material Systems and Structures*
Vol. 9, No 3, March, 1998
pp. 210 - 222.

*Keywords: smart structures, smart skin, switchmode amplifiers, power flow analysis, electrostrictive actuators, impedance matching*

## ABSTRACT

In this paper we analyze the power flow between stacked electrostrictor actuators and a pulse-width-modulated switching amplifier. The amplifier and actuator are analyzed as components of a smart skin whose function is underwater acoustic echo cancellation. An integrated model is developed with includes a dynamic structural model of the actuator, a dynamic model of the power electronics and a nonlinear electromechanical coupling mechanism of the electrostrictor actuation material. Using a linearized version of this model, the mechanical admittance of the actuator as seen by an external force is analyzed. It is shown that an outer acoustic control loop can modify this mechanical admittance and optimize the power coupling between the actuator and an external fluid medium by impedance matching. With the nonlinear model, the power flow between the electrical and mechanical systems is analyzed through simulation. The flow of power is traced from the power injected by the external force, through the amplifier and into the electrical bus. It is shown that effective power flow occurs only when the frequency of the external force is within the bandwidth of the amplifier. This analysis also reveals that the electrical power flow through the actuator is two orders of magnitude larger than the external mechanical power extracted by the actuator. This analysis shows that one main requirement on the amplifier design is to manage the charge flow through the actuator.

## INTRODUCTION

Smart materials or smart structures are materials that contain actuators, sensors, and control systems so that the smart structure can actively respond to its environment. The ideal smart structure would have only a power connection for the injection of energy and a data connection to control the flow of that energy. From one point of view, the function of the actuators is to inject or remove energy from the system. The function of the sensors and control system is to manage the flow of that energy. We adopt this view in this paper.

The analysis in this paper is motivated by the smart skin being developed for dual use as an acoustic echo cancellation device and for medical imaging (Bridger, et al., 1996). This smart skin employs stacked electrostrictor actuators mounted on a rigid base. A headmass is mounted on the actuators. A PVDF sensor attached to the headmass detects the incoming acoustic wave and produces a feedback signal for the digital control system. The controller provides a command signal for the power amplifier that drives the actuators. The actuators vibrate the headmass and generate a canceling acoustic wave. The only external connections on this smart skin are the electrical connection to the power bus and the data line for external monitoring of the digital processing.

Consider the flow of energy through this smart skin. Electrical energy is supplied to the smart skin from the electrical power bus. This electrical power is conditioned and controlled by the power amplifiers and delivered to the electrostrictor actuators. These actuators act a transducers converting the electrical energy into mechanical energy. This mechanical energy then flows from the smart skin into the surrounding fluid as acoustic energy. An interesting aspect of this smart skin is that it also allows the energy to flow in the opposite direction, as we shall describe in detail in this paper.

There are several individual devices that control the power flow in this smart skin. One of the key devices is the power amplifier that takes the raw electrical power from the power bus and delivers it to the actuator in response to the command signal from the digital control system. The analysis of the power flow through this amplifier is a main focus of this paper. In order to understand this power flow it is necessary to understand where the power is coming from (the power bus characteristics), the where the power is going (the load provided by the actuator), and how the amplifier processes the power.

There are several amplifier topologies for driving electrostrictor actuators. These topologies include standard linear amplifiers, switched capacitor amplifiers, and switchmode amplifiers. In this paper we will focus on a bi-directional pulse width modulated (PWM) or switchmode amplifier (Zvonar, et al., 1996; Zvonar and Lindner, 1997a). This amplifier has a completely different topology from linear amplifiers. These switched mode amplifiers use a pair of MOSFET transistors as switches to connect the load directly to the power bus. This configuration allows for a bidirectional power flow between the actuator and the power bus with very small internal power losses in the amplifier. In this paper we will assume an ideal power bus which supplies a constant DC voltage, leaving further discussions as future work.

Electrostrictor actuators, the electrical load of the amplifier, are basically nonlinear capacitors. When they are driven with a sinusoidal signal, they circulate a large amount of charge between the actuator and amplifier. The primary task of the amplifier is to manage this charge flow, or power flow. In this paper we will show that the switchmode amplifier acts as a switch to channel the charge flow between the power bus and the actuator. Since this power is not dissipated as heat but returned to the power bus, this configuration allows for very efficient operation and compact size (Zvonar, et al., 1996). Standard amplifiers are designed to handle a one way flow of power from the power bus to the load. These amplifiers react to power returning from the load by dissipating it as heat. Hence, they tend to require a large heat sink because the amount of power returned to the amplifier from the actuator is quite large. Switched capacitor amplifiers, which are too complicated to discuss in detail here, are a blend of these two amplifier concepts.

To fully understand the power flow through the smart skin it is necessary to account for the power flow through the other components. Accordingly we employ simplistic models of the coupling between the actuator and structure and the acoustic coupling between the structure and the surrounding fluid. It is also important to include the control system, because the control system regulates the power flow through the amplifier by the amplifier command signal. The purpose of this paper is to demonstrate a method for power flow analysis, and to explain in detail how the amplifier interacts with the actuator. The inclusion of more realistic models for the coupling between the other components of the smart skin is straight forward but outside the focus of the paper.

The analysis in this paper is carried out using an integrated model of the amplifier and actuator (Lindner, DiGiorgi, and MacDermont, 1997). This model includes a nonlinear model of the electrostrictive actuation material (Hom, et al., 1994). The switchmode amplifier model described in these papers is a so-called averaged model (Sable, et al., 1990). The power flow analysis uses both a linearized and nonlinear model of the amplifier and actuator. (The linearized model is essentially equivalent to the models of Hagood, et al. (1990).) We begin by studying the impedance of the linear model. It is also shown that the most efficient power transfer between the electrical and mechanical subsystems occurs when the amplifier is operated within its bandwidth (Zvonar, et al. 1998). This result relates the amplifier frequency response to the mechanical admittance of the actuator and structure. Then we extend this linear analysis to the nonlinear system by simulating the instantaneous power signals in the system (Zvonar and Lindner, 1997b). It is shown that the electrical power flow through the actuator is two orders of magnitude greater than the electrical power generated in the

actuator by an external force acting on the actuator. This result demonstrates the importance of managing the charge flow in the amplifier. The nonlinear analysis also clearly demonstrates the reverse power flow from the impinging acoustic wave through the actuator and amplifier to the power bus. This analysis lends insight into the sizing and operation of the actuator and amplifier.

The electrostrictor actuators are similar to piezoelectric actuators in that they present a capacitive load to the amplifier. The results in this paper generalize to piezoelectric actuators. It is only necessary to account for the different nonlinearities of the piezoelectric material, and the differing electrical requirements in the amplifier and power bus design. It is expected that qualitatively similar results will be obtained. The electrical power requirements of piezoelectric actuators has been studied by Brennan and McGowan (1997) using linear models of the actuator and structure. They conclude that the electrical power requirements can be estimated from the effective capacitance, although experiments show that the power requirements exhibit strong nonlinear effects. These results are consistent with the results in this paper. Our analysis provides a nonlinear model for the power flow and quantifies the power flow from the structure back into the amplifier. While this reverse power flow may be negligible in some applications, in high power applications it may be significant.

The electrostrictive actuators take the electrical power and convert it to mechanical power. This mechanical power is transferred to the structure through the mechanical coupling between the actuator and structure. This aspect of the power flow has been studied using impedance concepts (Liang, Sun, and Rogers, 1994; Niezrecki and Cudney, 1994; Zhou and Rogers, 1995; and Flint, Liang, and Rogers, 1995). In this paper it is shown how the impedance of the amplifier enters into this analysis. Basically, maximum power flow is achieved only over the bandwidth of the amplifier. This result is supported by the nonlinear analysis.

This paper is organized as follows. First, a description of the smart skin, the amplifier, and actuators is given. Then the nonlinear model is derived and linearized. Next an impedance analysis is conducted. Finally, the power flow in the nonlinear model is analyzed.

## DESCRIPTION OF THE SMART MATERIAL

This paper is motivated by a smart skin developed for underwater echo cancellation. The smart skin would be composed of a dense layer of acoustic pistons each acting as an independent acoustic source. These acoustic pistons would be controlled in a coordinated way to cancel an incoming ping. We are interested a single acoustic piston shown in Figure 1.

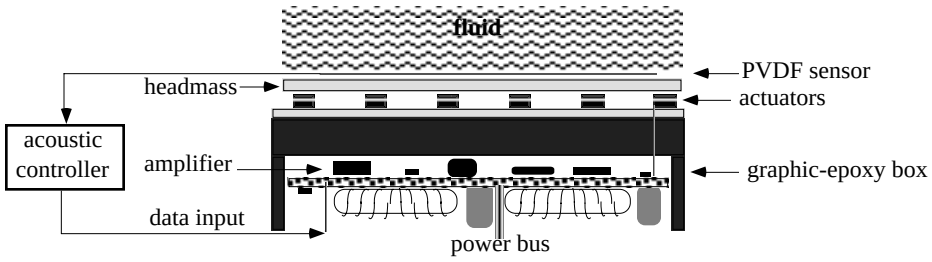


Figure 1 - Acoustic Piston

The acoustic piston is a 3" by 3" graphite-epoxy box, the top of which provides a rigid base for mounting thirty six (36) stacked PMN electrostrictor actuators. Attached to the top of the actuators is a rigid plate called the headmass. Four power amplifiers are mounted inside the box. Each amplifier is used to drive a group of nine (9) actuators When the actuators are vibrated, the headmass generates an acoustic wave.

These pistons are mounted on a baseplate. Also attached to the baseplate are the digital control electronics. A PVDF pressure sensor mounted on the headmass of each piston provides the feedback signal for detecting the incoming acoustic wave. The digital control electronics would

process all of the feedback signals, and provide control signals for the power amplifiers. The whole assembly is potted for protection against the water environment with only one external power bus connection and one external data connection.

The idea behind this smart skin is that when an acoustic wave strikes the skin, the pressure is sensed and that the sensor signal is sent to the controller. The control system generates an input signal to the power amplifiers. The power amplifiers deliver raw electrical power from the power bus to the actuators according to this control system input signal. The stacked electrostrictor actuators convert the electrical power into mechanical power. The mechanical response of the actuators causes a structural response (vibrations) in the headmass of the piston which in turn couples into the fluid. This coupling converts the mechanical power into acoustical power. If the system is designed properly, the outgoing acoustic wave should cancel the incoming acoustic wave.

In this paper we are not concerned with acoustic echo cancellation, but rather with understanding the basic principles of operation of the smart skin. We are generally concerned with the power flow in the smart skin, and in particular, with the power flow from the electrical bus into the actuators. The method of analysis, however, can be applied to other smart structures.

## DESCRIPTION OF THE ACTUATORS AND AMPLIFIER

The four (4) power amplifiers contained in each piston are shown in Figure 2.

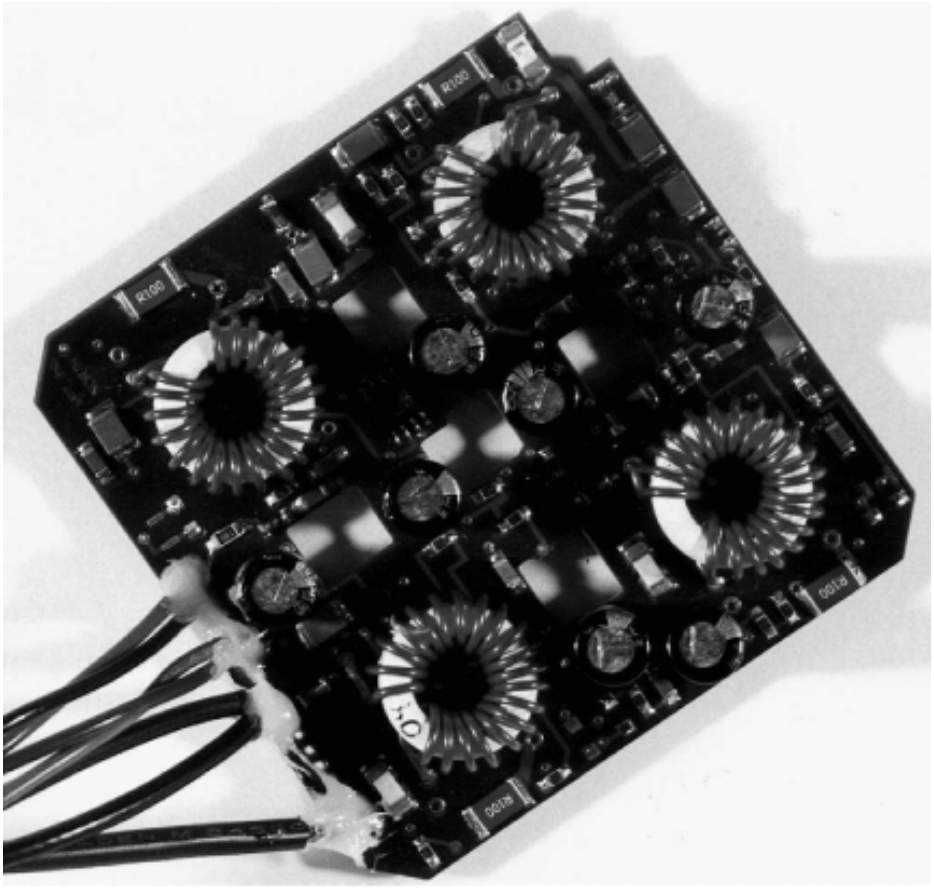

Figure 2 - Four Switchmode Amplifiers

The specifications for each amplifier are given in Table 1.

**Table 1 Amplifier Specifications**

| | |
|---|---|
| Input Voltage | 32 Vdc |
| Output Voltage | 22 Vpp with 14 Vdc bias |
| Output Current | 3.1 App |
| Size | 2.8" x 2.8" x 0.5" |
| Weight | 4.3 g |

Each of the four amplifiers drive nine (9) actuators of the 36 actuators on each piston. Each group of nine stacked PMN actuators are connected in parallel. A simplified circuit diagram of the switchmode amplifier that drives these actuators is shown in Figure 3. (In this figure the group of nine actuators is shown as one actuator.)

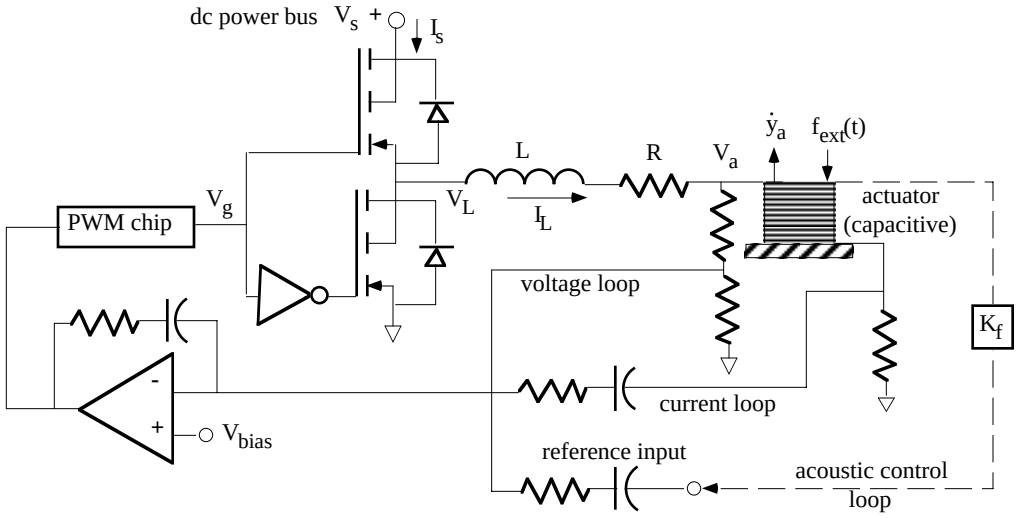


Figure 3 - Simplified Diagram of the Amplifier and Actuator

The purpose of this amplifier is to drive the actuators so as to generate an acoustic wave to cancel the incoming acoustic wave. A frequency band of interest is specified by a minimum and maximum frequency; the minimum frequency is above DC. We call this frequency band the *frequency band of interest.*

Each chiplet actuator is a stacked PMN device approximately h = 2.1 mm tall with a base 3.6 mm by 4.6 mm. It consists of $N_c$ = 78 layers where each layer is separated by a distance d = 25 μm. These layer are connected in parallel to form an equivalent single capacitor. The actuators are also connected in parallel. The total nominal capacitance of all nine actuators is approximately 45 μF. (Below we will use a nonlinear model of the actuation material, however.) Because these actuators are composed of an electrostrictor material, they are operated about a 14 Vdc bias. In this particular application, these actuators are operated significantly below their mechanical resonance. At the low end of the frequency band of interest, the actuation material is driven into electrical saturation.

The power amplifier driving the actuators is based on a buck switchmode DC to DC power converter as shown in Figure 3. The amplifier is driven by a 32 V DC power bus. This DC voltage is chopped by the two MOSFET power transistors which are driven in a complementary mode. The gate drive signal, $v_g(t)$, to the MOSFET transistors is a fixed frequency square wave with a variable duty cycle, $d_c(t)$. The gate drive signal is generated by the PWM chip which determines the frequency of the square wave. This frequency is called the switching frequency, and it is an order of magnitude above the highest frequency in the frequency band of interest. Since the MOSFET transistors are either in their fully on or off state, the voltage on the MOSFET side of the inductor, $v_L(t)$, is also a square wave with the same duty cycle as the gate drive voltage with a peak voltage equal to the bus voltage. The inductor and actuators (capacitors) act to filter out the unwanted harmonics in the square wave to produce a (essentially) constant voltage across the actuators which is proportional to the duty cycle of the gate voltage. The current and voltage contain a first harmonic at the switching

frequency. The magnitude of this harmonic depends on the size of the inductor. In the amplifier model used below, the switching effects of the transistors are ignored. The higher order harmonics of the actuator voltage and current are filter out with the inductor and capacitor (actuator). The duty cycle is assumed to be proportional to the control loop signals summed with the reference signal. This model is the so-called average model of the switching electronics.

This amplifier employs two control loops which adjust the duty cycle of the gate voltage based on the voltage across the actuators (voltage loop) and the current delivered to the actuators (current loop). The purpose of the voltage loop is to maintain a constant bias voltage on the actuator at DC through the use of an integrator. The purpose of the current loop is to control the current entering the actuator to be proportional to an external reference voltage, $i_{ref}(t)$. The transfer function from the external reference voltage to the current into the actuators, $i_L(t)$, is a bandpass filter which is flat in the frequency band of interest as shown in Figure 4.

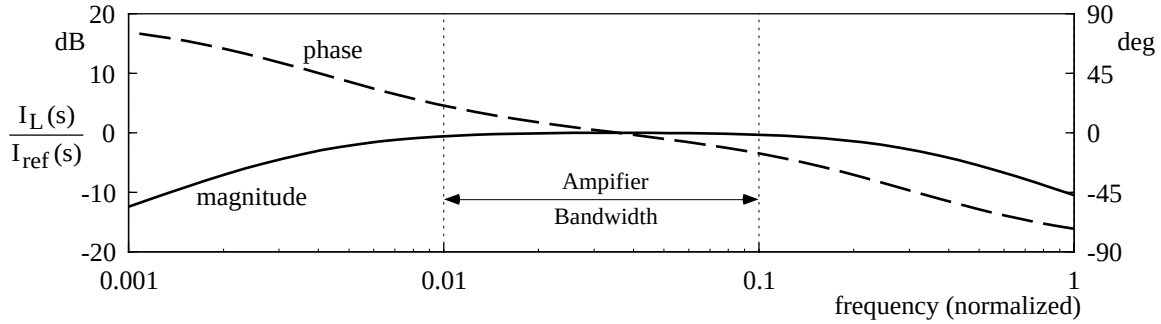


Figure 4 - Transfer Function from Amplifier Input, $I_{ref}$, to Actuator Current, $I_L$

In other words, the control system is designed so that a sinusoidal reference signal will cause sinusoidal current flow regardless of the voltage variations across the actuator. This amplifier is current controlled. Current control has been shown to mitigate the effects of the actuator material nonlinearities (Zvonar and Lindner, 1997). It can also be seen from the analysis below that the current into the actuator is proportional to the velocity of the top of the actuator. Since velocity is the natural variable to control for acoustic echo suppression, a current controlled amplifier is natural for this application.

In this paper we will take a slightly different view of these control loops in the amplifier. The purpose of this paper is to investigate the power flow through the amplifier and the actuator. The main electrical power flow though the amplifier is through the MOSFET transistors and the inductor into the actuators. The actuators transform energy between electrical and mechanical form. From this power flow viewpoint, the control loops act as energy switches to modulate the flow of power between the electrical and mechanical system. The amplifier reference signal is generated by the acoustic control system from the PVDF pressure sensor signal. In particular, the external reference signal serves to determine the power coupling between the power bus and the actuators. This idea will be explored below.

In the discussion below, we will use the acoustic control loop in Figure 3 in the investigation of the power flow through the amplifier and actuator. For this analysis we assume that this feedback is given by

$$i_{ref}(t) = K_f f_{ext}(t) \tag{1}$$

where $K_f$ is the feedback gain. For the purposes of this paper we will make a very simple assumption. To achieve perfect cancellation, we want to generate an acoustic wave which is 180° out of phase from the incoming wave. Therefore, we want the velocity of the piston head to be 180° out of phase with the pressure of the incoming wave. Assuming that the transfer function between the amplifier reference input signal and the velocity at the top of the actuator is a pure gain, then the acoustic control loop is just negative gain feedback. We will use this feedback in the analysis below.

In the switchmode amplifier one of the MOSFET transistors is always on, and one is always off. Hence, the inductor is either connected to the high side of the power bus or to ground. As a first approximation, we can assume that the MOSFET transistor in the on mode presents essentially zero resistance between the power bus and inductor. Hence, the amplifier imposes very little impedance between the actuator and the power bus, essentially allowing the power to flow freely back onto the power bus. This type of operation is very different from that of a conventional Class A or B amplifier. These amplifiers typically dissipate a significant amount of power as conduction losses in the transistors themselves which, in turn, is dissipated in heat. Switchmode amplifiers are attractive where power losses and thermal management are critical.

In this paper we are mainly concerned with the power flow between the power bus and the fluid. There are several sources of power loss within the amplifier and the actuator which are ignored. These sources of power loss in the amplifier include: the losses in the discrete components (resistors and capacitors), conduction losses in the MOSFETs, and high frequency losses in the inductor, the MOSFET and its diode. In addition, there are some fixed overhead electrical power losses in the PWM controller chip. There are some power losses in the actuation material itself, but for electrostrictor material these are relatively small because of its low hysteresis. All of these losses can be ignored for the smart material we are considering here because they represent a relatively small fraction of the total power flow.

## DERIVATION OF THE MODEL

In this section we will develop the model of the amplifier and actuators that we will use in the subsequent analysis. The development is divided into two parts. The first part develops the model of the inductor and the actuator. We can think of these two components as being extracted from the larger system in Figure 3. This model development follows a standard energy method development. Then the rest of the amplifier is integrated into the existing model using the averaging concepts associated with switchmode amplifiers.

We consider first the actuators. These actuators are rigidly attached to the base of the piston which is considered rigid. We assume that a uniform force is applied to the top of all of the actuators causing them to compress uniformly. Hence, we can treat these nine actuators as a single mechanical unit with an effective area of A and height h. If Y is Young's modulus of the actuation material, then the effective stiffness is

$$k_a = \frac{YA}{h}. \tag{2}$$

The total mass of the actuators is $m_a$ and the damping coefficient of the actuators is $c_a$. The displacement of the top of the actuator is given by $y_a(t)$.

Electrically, each of these stacked actuators are essentially a stack of $N_c$ capacitors wired in parallel. Furthermore, the actuators are all wired in parallel. So the amplifier sees an equivalent capacitor with a plate area of $A_e = (N_c)(A)$ and a separation of d. (Hence, $h = (d)(N_c)$.)

Following Hom, et al. (1994) we assume that the constitutive equations of the PMN material are given by

$$\begin{aligned} \varepsilon &= \frac{\sigma}{Y} + Q_{11}P^2, \\ E &= -2Q_{11}P\sigma + \frac{1}{k}\tanh^{-1}\left(\frac{P}{P_s}\right) \end{aligned} \tag{3}$$

where the polarization, P, and stress, $\sigma$, are the independent variables and strain, $\varepsilon$, and electric field, E, are the dependent variables. The constants $Q_{11}$, k, and $P_s$ are determined by the material. To relate these constitutive equations to variables of the amplifier, define the voltage across the actuators

as $v_a(t)$ and the charge in the actuators as q(t). Taking into account the geometry of the actuators, and recognizing that polarization is charge per area, electric field is voltage per distance, and strain is displacement per length, using (3) the expression for the voltage across the actuator in terms of displacement and charge is

$$v_a(t) = dE(t) = -2dQ_{11}\left(\frac{q(t)}{A_e}\right)\left[Y\frac{y_a(t)}{h} - Q_{11}Y\left(\frac{q(t)}{A_e}\right)^2\right] + \frac{d}{k}\tanh^{-1}\left(\frac{q(t)}{P_s A_e}\right). \tag{4}$$

Now we can write the model of the amplifier coupled to the actuators. The mechanical potential and kinetic energies of the actuators are given by

$$PE_m = \frac{1}{2}k_a y_a^2, \quad KE_m = \frac{1}{2}m_a \dot{y}_a^2 \tag{5}$$

Referring to Figure 3, the electrical potential energy in the capacitor is

$$PE_e = \int v_a dq. \tag{6}$$

and the electrical kinetic energy in the inductor is

$$KE_e = \frac{1}{2}Li_L^2. \tag{7}$$

With these definitions of the energy in the system, we can define the Lagrangian as

$$L = KE_e + KE_m - PE_e - PE_m. \tag{8}$$

Taking into account the nonconservative forces in Figure 3, the dynamic equations follow from

$$\begin{aligned} \frac{d}{dt}\left(\frac{\partial L}{\partial \dot{y}_a}\right) - \frac{\partial L}{\partial y_a} &= f_{ext} - c_a \dot{y}_a \\ \frac{d}{dt}\left(\frac{\partial L}{\partial \dot{q}}\right) - \frac{\partial L}{\partial q} &= v_L - Ri_L \end{aligned} \tag{9}$$

where $f_{ext}(t)$ is the external force acting on the actuator and R is the series resistance of the inductor in Figure 3. Performing the calculations indicated in Equation (9) we obtain the dynamic equations

$$\begin{aligned} &m_a \ddot{y}_a(t) + c_a \dot{y}_a(t) + k_a y_a(t) = f_{ext}(t) + k_a N_c dQ_{11}\left(\frac{q(t)}{A_e}\right)^2, \\ &L\ddot{q}(t) + R\dot{q}(t) + \frac{d}{k}\tanh^{-1}\left(\frac{q(t)}{P_s A_e}\right) + v_t(t) = v_L(t), \end{aligned} \tag{10}$$

where

$$v_t(t) = -2dQ_{11}\left(\frac{q(t)}{A_e}\right)\left(\frac{N_c}{A_e}\right)\left[k_a y_a(t) - k_a N_c dQ_{11}\left(\frac{q(t)}{A_e}\right)^2\right]. \tag{11}$$

If we compare (11) to (4) we see that the actuator voltage, $v_a(t)$ is equal to (after some manipulation)

$$v_a(t) = \frac{d}{k}\tanh^{-1}\left(\frac{P(t)}{P_s}\right) + v_t(t) = \Psi(P) + v_t(t). \tag{12}$$

This analysis has ignored the fluid loading on the piston. This assumption is for the sake of simplicity since our focus is on the power flow through the amplifier and actuator. Including fluid loading on the piston would not change the character of the analysis.

To the model in Equation (10) we must add the control loops. The average model of the switching electronics says that the positive voltage on the inductor is given by the product of the duty cycle, $d_c(t)$, times the bus voltage, $V_s$; that is,

$$v_L(t) = d_c(t)V_s. \tag{13}$$

Similarly the power bus current, $i_s(t)$, is given by

$$i_s(t) = d_c(t)i_L(t). \tag{14}$$

(The bus voltage and current play a central role in the analysis of the power flow given below.) The duty cycle is regulated by the control loops. The controller is given by

$$d_c(t) = K_{pm}\left[K_i\left(i_{ref}(t) - i_L(t)\right) + \frac{K_v}{s}\left(V_{bias} - v_a(t)\right)\right]. \tag{15}$$

The gain $K_{pm}$ is the gain of the PWM chip. The voltage control loop gain is $K_v$. This loop serves to keep the DC bias voltage, $V_{bias}$, across the actuator at its nominal value through the use of integral control. The current control loop gain is $K_i$. The function of the current control loop is to ensure that the current through the inductor, $i_L(t)$, follows the external reference signal, $i_{ref}(t)$, in the bandwidth of the amplifier.

Equations (10) through (15) represent a dynamic coupled model of the amplifier and the actuator. These equations are embedded in the block diagram shown in Figure 5.

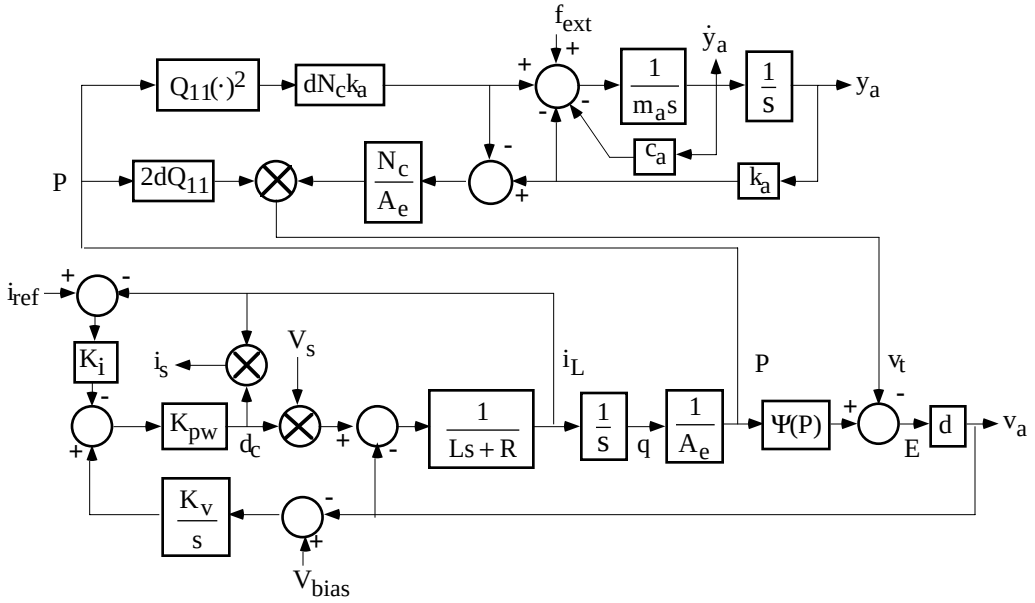


Figure 5 - Block Diagram of Nonlinear Model

This model is validated by experiment by Zvonar, et al. (1996). It can be shown that this system is globally, asymptotically stable. These results will be reported elsewhere.

## MODEL LINEARIZATION

We now derive a linear model of the system by linearizing the system equations about an operating point. This linear model will allow us to compute impedance transfer functions to calculate power flow. The operating point of the system is determined by the actuator bias voltage, $V_{bias}$, and with no external force on the actuator. This equilibrium point is found by setting the derivatives in the model equal to zero. Equation (10) becomes

$$Y_a = N_c dQ_{11}\left(\frac{Q}{A_e}\right)^2, \tag{16}$$

$$\frac{d}{k}\tanh^{-1}\left(\frac{Q}{A_e P_s}\right) + V_t = V_L \tag{17}$$

and Equation (11) becomes

$$V_t = -2dQ_{11}\left(\frac{Q}{A_e}\right)\left(\frac{N_c}{A_e}\right)\left[k_a Y_a - k_a N_c dQ_{11}\left(\frac{Q}{A_e}\right)^2\right]. \tag{18}$$

(Notation: The upper case letters represent the equilibrium values of time varying quantities.) Substituting the equilibrium value of position, $Y_a$, in Equation (16) into Equation (18) we see that that the equilibrium value for $v_t(t)$ equals zero, $V_t = 0$. Finally, we note that in equilibrium the actuator voltage is equal to the constant bias voltage which is also equal to the inductor voltage, $V_a = V_{bias} = V_L$ as can be seen from (17) and (12). In steady state, a constant voltage across the actuator will cause the capacitor to fully charge. In this state, no current will flow into the actuator, resulting in no net voltage drop across the resistance in the inductor.

The nonlinear dynamic equations in Equation (10) when linearized about this equilibrium point become

$$\begin{aligned} &m_a\ddot{\tilde{y}}_a(t) + c_a\dot{\tilde{y}}_a(t) + k_a\tilde{y}_a(t) = f_{ext}(t) + \frac{2k_a N_c dQ_{11}Q}{A_e{}^2}\tilde{q}(t), \\ &L\ddot{\tilde{q}}(t) + R\dot{\tilde{q}}(t) + \frac{d}{kA_e Ps}\frac{1}{1-\left(\frac{Q}{A_e P_s}\right)^2}\tilde{q}(t) + v_t(t) = \tilde{v}_L(t) \end{aligned} \tag{19}$$

where $v_t(t)$ is equal to

$$v_t(t) = -\frac{2k_a N_c dQ_{11}Q}{A_e^2}\tilde{y}_a(t) + \frac{1}{k_a}\left(\frac{2k_a N_c dQ_{11}Q}{A_e^2}\right)^2\tilde{q}(t). \tag{20}$$

(Notation: The tilde represents the linearized variable when its equilibrium value is non-zero.)

These equations can be simplified by making the definition

$$\Theta = \frac{2k_a N_c dQ_{11}Q}{A_e{}^2} \tag{21}$$

where $\Theta$ is an electromechanical conversion constant at the bias voltage and

$$\frac{1}{C} = \frac{d}{kA_eP_s}\frac{1}{1-\left(\frac{Q}{A_eP_s}\right)^2} + \frac{\Theta^2}{k_a}. \tag{22}$$

where C is the effective (clamped) capacitance of the actuator at the bias voltage. Substituting Equations (21) and (22) into Equations (19) and (20) we get the linearized model

$$m_a\ddot{\tilde{y}}_a(t) + c_a\dot{\tilde{y}}_a(t) + k_a\tilde{y}_a(t) = f_{ext}(t) + \Theta\tilde{q}(t) \tag{23}$$

$$L\ddot{\tilde{q}}(t) + R\dot{\tilde{q}}(t) + \frac{1}{C}\tilde{q}(t) = v_L(t) + \Theta\tilde{y}_a(t). \tag{24}$$

This model is equivalent to the model of Hagood, et al. (1990). From Equation (24) (which is just the voltage drop across the power stage of the amplifier) we find that the actuator voltage is just

$$\tilde{v}_a(t) = \frac{\tilde{q}(t)}{C} - \Theta\tilde{y}_a(t). \tag{25}$$

Equations (23) through (25) together with the amplifier control Equations (13) and (15) comprise the linear model. A block diagram of the linearized system is shown in Figure 6.

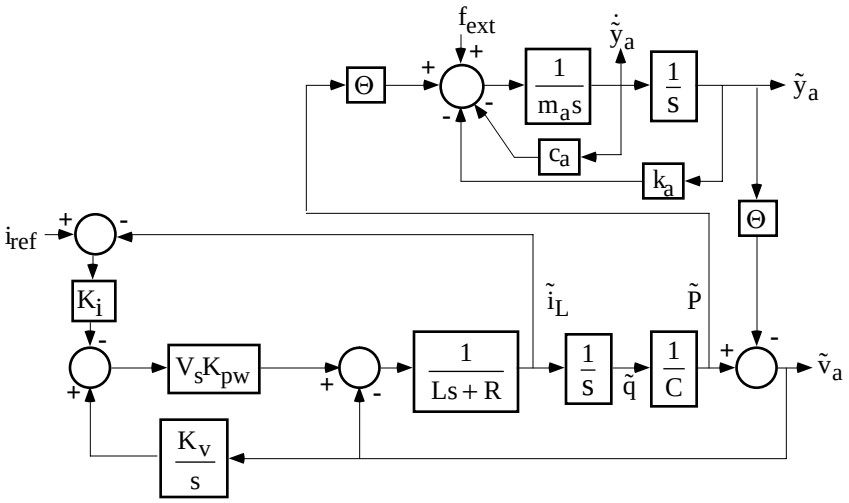


Figure 6 - Block Diagram of Linearized Model

## IMPEDANCE CALCULATION

In this section we will begin the analysis of the power flow through the amplifier and actuator using the linear model of the system derived in the last section. With a linear model we can use the idea of impedance matching to study the power flow through the system. The idea is to match the mechanical impedance at the actuator to the impedance of the fluid. This impedance match will maximize the coupling of the power into the fluid thereby maximizing our effectiveness to cancel the incoming acoustic wave (c.f. Liang, Sun and Rogers, 1994; Niezrecki and Cudney, 1994). To that end we calculate the mechanical impedance, or admittance, seen by the acoustic wave. This admittance is defined as the transfer function

$$\frac{\dot{Y}_a(j\omega)}{F_{ext}(j\omega)} \tag{26}$$

This transfer function can be calculated from the block diagram in Figure 6. From this block diagram, we see that the admittance in Equation (26) depends on the acoustic feedback control loop in (1). This control loop is indicated in Figure 3. It enters into the block diagrams in Figures 5 and 6 in an obvious way.

Figure 7 shows a plot of the real portion of the mechanical admittance in Equation (26) with the gain of the acoustic control loop taking both zero and nonzero values.

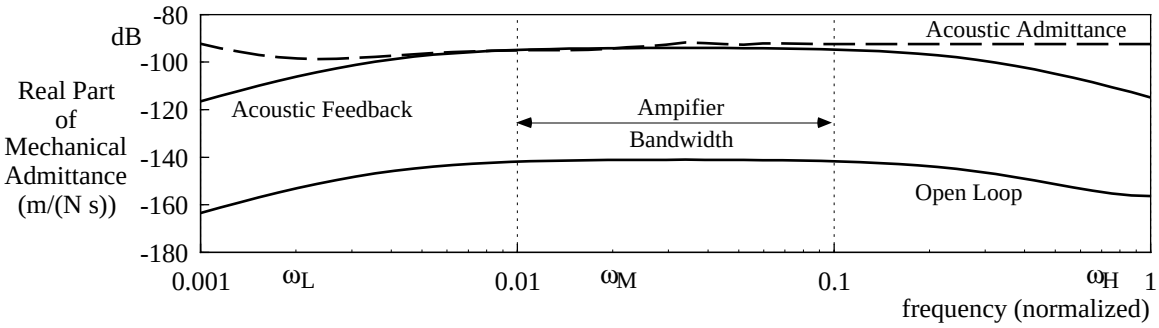


Figure 7 - Real Part of Mechanical Admittance

Also shown in Figure 7 is the acoustic admittance as seen by an equivalent circular piston in water (Kinsler, et al. 1982). For our analysis here, the exact shape of this acoustic admittance is not important, as we are illustrating the method of analysis and focusing on the interaction of the amplifier and actuator. The acoustic coupling between the piston and the surrounding fluid is a separate issue.

Figure 7 shows that the acoustic feedback control loop controls the mechanical admittance. Figure 7 clearly shows that by varying the gain of the acoustic controller from zero to a positive value, power transfer can be increased dramatically. This behavior can be explained as follows. When the acoustic feedback gain is zero, the reference input signal to the amplifier is always zero. This reference input signal is telling the amplifier to transmit zero power to the actuator. If fact, the stress feedback inherent in the actuation material is coupling some mechanical power back into the amplifier control loops. (See the block diagram in Figure 6.) Hence, some real power is being transmitted to the actuator and the admittance is not zero for zero gain on the acoustic controller.

When the acoustic feedback gain is changed from zero, the reference signal into the amplifier becomes a sinusoid at the frequency of the impinging acoustic wave. The reference signal causes power flow between the power bus and the actuator increasing the real power flow into the fluid. This increased power coupling is shown by the increase in the real part of the admittance in Figure 7. The reference signal is acting as an energy switch controlling the power flow between the amplifier and actuator. By adjusting the feedback gain we can match the mechanical admittance of the actuator/amplifier to the admittance of the fluid (also shown in Figure 7) thus maximizing the power flow to the fluid.

Also note that the power flow is highly frequency dependent. The real part of the mechanical admittance looking into the actuator shown in Figure 7 is a combination of the actuator dynamics and amplifier dynamics. While the exact relationship is rather complicated, the shape of the admittance in Figure 7 is quite similar to the shape of the frequency response function of the amplifier in Figure 4. Within the amplifier bandwidth we achieve maximum power transfer. Outside the amplifier bandwidth, the power transfer is degraded.

## POWER SIGNALS

### Definitions

The impedance analysis above demonstrates the power coupling between the amplifier and actuator and the surrounding fluid. It is also instructive to investigate the power flow within the amplifier and actuator. To do this analysis we need to define the power flow from the signals within the system. Unlike the impedance analysis, for this analysis we will use the nonlinear model of the actuator and amplifier. For the electrical signals, the instantaneous power is defined as the product of voltage and current. For the mechanical signals, power is defined as the product of force and velocity. Under steady-state conditions, a net mechanical power flow (the DC portion) must be balanced by a net electrical power flow.

On the mechanical side, the power supplied by an external force acting on the actuator, $P_{mi}$, is

$$P_{mi} = \dot{y}_a(t) f_{ext}(t) \tag{27}$$

which is the product of the velocity of the actuator and the applied force. Another mechanical power signal is the power from the conversion of electrical energy to mechanical energy. This power, called here the electromechanical power, $P_{em}$, is given by

$$P_{em} = \dot{y}_a(t)\left[k_a N_c d Q_{11}\left(\frac{q(t)}{A_e}\right)^2\right] \tag{28}$$

which is the product of the velocity of the actuator and the internally generated force in the actuator due to the charge applied to the actuator.

On the electrical side, we have the power supplied to the amplifier by the power bus, $P_{ei}$, which is the product of the bus voltage and current. From Figure 5 it can be seen that the power bus current, $i_s(t)$, is equal to the inductor current, $i_L(t)$, times the duty cycle, $d_c(t)$. The voltage associated with this current is the bus voltage, $V_s$. Hence, the power delivered by the power bus is

$$P_{ei} = V_s i_s(t) = V_s d_c(t) i_L(t). \tag{29}$$

The electric power consumed by the actuator, $P_{eo}$, is

$$P_{eo} = v_a(t) i_L(t) \tag{30}$$

which is the actuator voltage times the current flowing into the actuator. From the expression for the actuator voltage in (12), the power in (30) can be broken into two parts

$$P_{eo} = P_{ec} + P_{et}. \tag{31}$$

The first term $P_{ec}$ contains the field-polarization nonlinearity and is the "capacitive" portion of the actuator electrical power

$$P_{ec} = \left[\frac{d}{k}\tanh^{-1}\left(\frac{q(t)}{A_e P_s}\right)\right] i_L(t). \tag{32}$$

The first term in Equation (32) is the voltage developed across the actuator plates due to the charge q(t). The second term of the actuator power, $P_{et}$, which originates from the converse electrostrictive effect, will be called the transfer power. The transfer power is defined as

$$P_{et} = \left[ -2dQ_{11}\left(\frac{q(t)}{A_e}\right)\left(\frac{N_c}{A_e}\right)\left( k_a y_a(t) - k_a N_c dQ_{11}\left(\frac{q(t)}{A_e}\right)^2 \right)\right] i_L(t) \tag{33}$$

where we have used (11). The first term in (33) is the voltage developed across the actuator plates due to the net internal stress in the actuator (i.e., the converse effect in the constitutive equations). Note that the signals defining these power definitions are clearly identified in the block diagram in Figure 5.

**In-Band Analysis**

To explain how the amplifier controls the power flow to the actuator, we will examine the power flow through the amplifier and actuator with the help of the power signals identified above. This acoustic wave will generate a force on the actuator of the form

$$f_{ext}(t) = A\sin(\omega_i t). \tag{34}$$

The PVDF sensor will provide a feedback signal to the acoustic controller which will in turn provide a reference input to the amplifier that is a sinusoid of the same frequency as Equation (34). This sinusoidal reference signal will, in turn, cause the amplifier and actuator to respond. Using this external forcing signal we simulate the various signals in the system using the nonlinear model in Figure 5 with the acoustic control loop closed. The amplitude of the external force in Equation (34) is chosen so that the amplifier was driven at maximum voltage swing. The frequency of the external force in this subsection is in the passband of the amplifier as identified in Figure 7 as $\omega_M$. From the signals in the simulation we will calculate the power signals defined above. Note that the system is nonlinear, so the simulated signals will be non-sinusoidal even though the external forcing signal is sinusoidal.

We begin with the mechanical power flowing into the actuator. Figure 8 shows the velocity of the actuator and the applied external force.

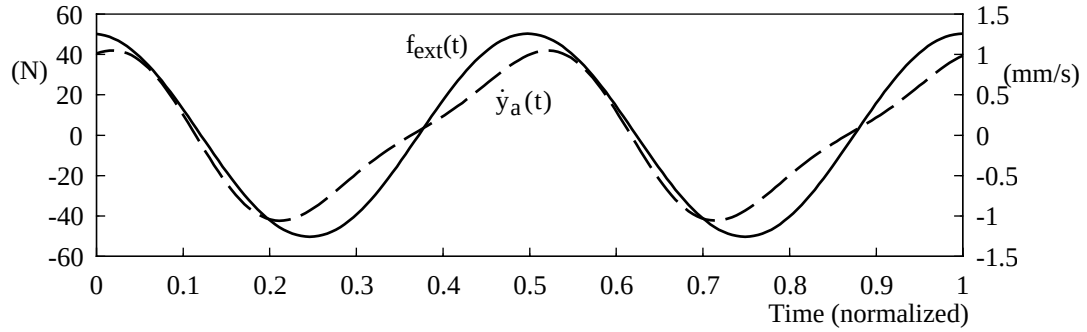


Figure 8 - Velocity of Actuator and External Force on Actuator

Notice that the velocity in Figure 8 is non-sinusoidal because of the quadratic relationship between the polarization and strain in the actuator. Also notice that the velocity and external force (Figure 8) are in phase. The fact that these two signals are in phase implies that there is a net power flow into the actuator and out of the incoming acoustic wave. This net power flow can be seen by examining the mechanical power signals which are shown in Figure 9. We see that the mean value of $P_{mi}$ in Figure 9(a) is positive. The positive mean value implies a net loss of power from the incoming acoustic wave. Since the mechanical losses in the actuator are zero in this simulation, this power is being consumed by the actuator by converting this mechanical power into electrical power. We will trace this power by examining the electrical power signals.

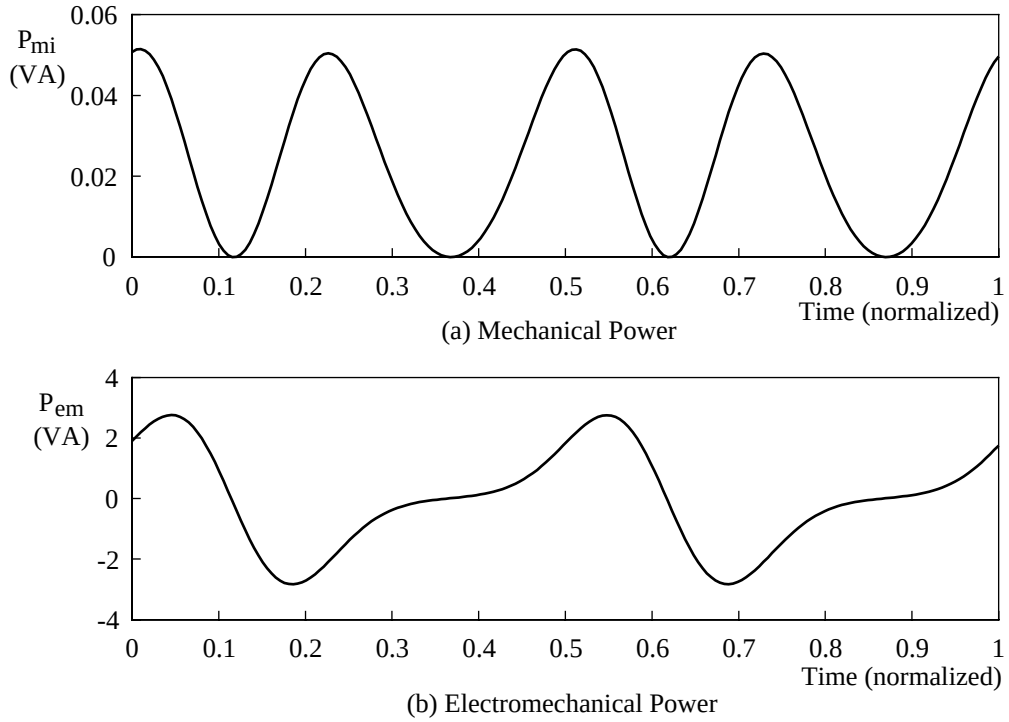


Figure 9 - Mechanical Power Flow (In-Band)

We also see that the electromechanical power, $P_{em}$, in Figure 9(b) is much larger than mechanical input power, $P_{mi}$, in Figure 9(a). Even though the mean value of the electromechanical power equals the mean value of the mechanical input power (power balance), we have a much larger reactive component in the electromechanical power. This power represents cyclic conversion between mechanical and electrical power as energy stored in the internal stiffness of the actuator and then returned back to electrical energy. This cycling of electrical energy can be seen by examining the voltage and current in the actuator shown in Figure 10.

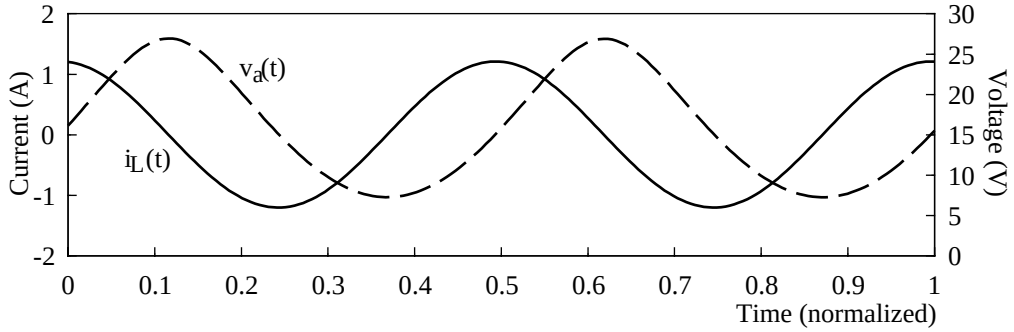


Figure 10 - Actuator Voltage, $v_a(t)$ and Actuator Current, $i_L(t)$

Since the amplifier is configured to control current, the actuator current in Figure 10 is sinusoidal like the externally applied force, but the voltage in Figure 10 is non-sinusoidal. The voltage is not sinusoidal due to the nonlinear relationship between the electric field in the actuator and its polarization. Also notice that the voltage and current are out of phase. Because these signals are out of phase, most of the power in the actuator is reactive. This cycling of electrical power can be seen by examining the electrical power signals in Figure 11.

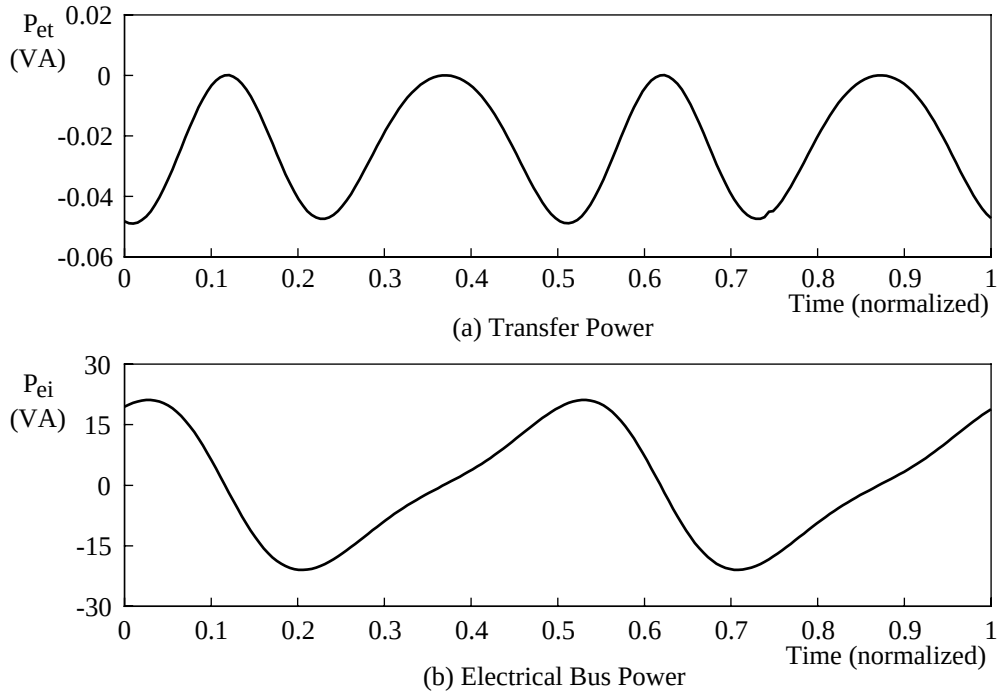


Figure 11 - Electrical Power Flow (In-Band)

When we compare the transfer power in Figure 11(a) with the mechanical input power in Figure 9(a), we see a resemblance. As mechanical power is dissipated on the mechanical side, it must appear on the electric side. The transfer power represents the power which is converted from mechanical to electrical power. The sign of the mean value of the transfer power (negative) indicates that power is flowing from the mechanical to the electrical side of the actuator.

Since the actuator is transforming the mechanical power into electrical power, this electrical power is then carried by the amplifier back onto the power bus. This power transport can be seen by examining the electrical power flow in the power bus. The mean value of the bus power, $P_{ei}$, in Figure 11(b), is -20mW. Although relatively small, this power flow is still negative. A negative mean bus power implies a net power flow is back onto the power bus. Furthermore, this net power flow is equal to the power entering the amplifier from the actuator via the transfer power. In other words, we have tracked the power from its removal from the acoustic wave through the actuator and amplifier and into the power bus.

We see that the electrical bus power in Figure 11(b) is much larger than the transfer power generated in the actuator in Figure 11(a). The majority of the electrical power flowing through the amplifier is reactive in nature. A large amount of charge is being cycled in and out of the actuator to carry out the electrical power generated by the actuator in response to the applied external force. This behavior is characteristic of electrostrictor and piezoelectric materials which are capacitive in nature. The power amplifier for these actuator materials has to be designed to manage this charge movement. The switchmode amplifier simply returns this charge to the power bus. For an electric power bus with a storage component, this energy can be stored for use on the next cycle. One convenient way to store this charge is to put a storage capacitor on the amplifier power bus input.

If a linear amplifier were used in this application instead of a switching amplifier, the power bus would still deliver power to the amplifier when the power flowed from the amplifier to the actuator. However, when the power flowed from the actuator back into the linear amplifier, this portion of the power would be dissipated as heat. Hence, linear amplifiers, while having many desirable properties, would require a large heat sink in this application. Furthermore, the total system power requirement would increase significantly since much power would be lost in the heat sink.

The large amount of electrical power being cycled into the electrostrictor actuators is required primarily to generate enough stroke in the actuators to produce an acoustic wave in the fluid. Most of the power is being used to supply a force that is not used. This analysis suggests that the force/stroke characteristics of the actuator are mismatched for this application.

The above analysis shows how the switchmode amplifier manages the electrical power flow for frequencies within the bandwidth of the amplifier. The key power signal is the transfer power. This signal shows the power that is being transferred from the actuator back into the amplifier and out into the power bus. This power signal represents the essential action of the actuator while the other power signals show the energy cycling in the system. This power transfer is accomplished because the amplifier is designed for the electrical load presented by the actuator in this frequency band.

**Out of Band Analysis**

Next we will trace the power flow when the amplifier is not used in the frequency band for which it is designed. This analysis will illustrate what happens when the amplifier is not properly matched to the actuator. Again we will assume an external forcing signal of the form in Equation (34). We will determine the transfer power for three different excitation signals. The first frequency, $\omega_L$, is below the bandwidth of the amplifier. The second frequency, $\omega_H$, is above the bandwidth of the amplifier. These signals are identified in Figure 7. We say these frequencies are out of band. The third frequency, $\omega_M$, is in-band and equal to the frequency used in the previous subsection. The amplitude of the external forcing signal is equal for all three frequencies. The amplitude of the external force used in this subsection is lower than the amplitude of the external force used in the last subsection, however. This change was required because the amplifier is not designed to operate out of the frequency band of interest. Lowering the external force amplitude will lower the power amplitudes, however, a comparison of the relative amplitudes for the three frequencies introduced above can still be accomplished.

Figure 12 shows the transfer power for the actuator excited by an external force with these three frequencies.

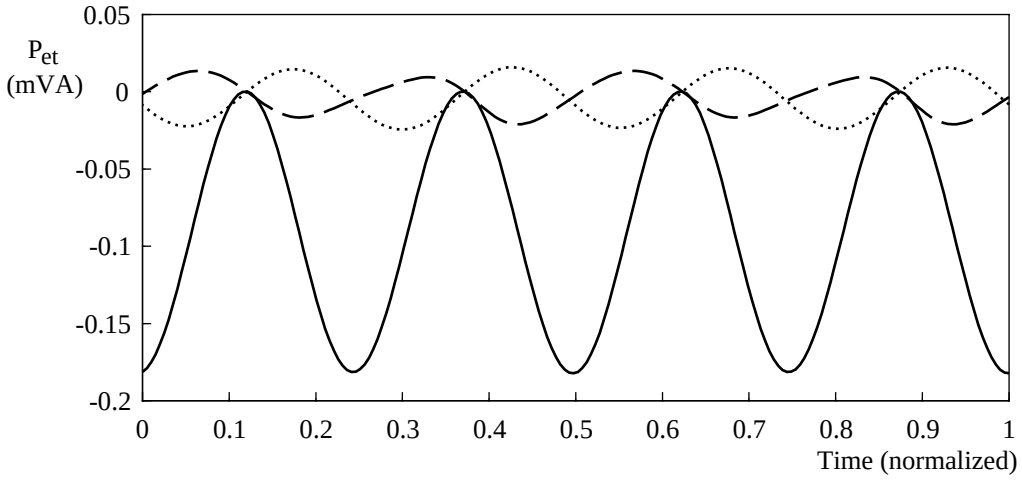


Figure 12 - Nonlinear Simulation of Transfer Power

Figure 12 should be interpreted in the following way. The time axis is normalized *to each signal separately*. If these three signals were graphed in the same time scale, they would have dramatically different frequencies, and comparison would be difficult.

The transfer power in Figure 12 clearly shows the degradation of the performance of the amplifier and actuator outside of the amplifier bandwidth. First, compare the mean power transfer when the frequency of the external force excitation signals is in-band and out of band. When the excitation frequency is in-band, the transfer power is purely negative indicating that power is always

being extracted from the acoustic wave. When the excitation frequency is out of band, the transfer power is both positive and negative. Here the power is being pumped into the fluid, as well as being extracted from the acoustic wave. There is a local cycling of power in the actuator. This situation is undesirable.

Second, compare the mean values of the transfer power signals for in-band and out of band excitation frequencies. The mean value for the in-band case is -90μW. The mean value for the below band case is -3.1μW and the mean value of the above band case is -4.2μW. When the amplifier is excited by reference signals which are out of the amplifier's bandwidth, the total amount of power which is extracted from the acoustic wave is reduced.

Suppose the frequency of the external force (acoustic wave) is outside the amplifier's bandwidth. The acoustic control loop produces a reference signal to the amplifier that is in phase with the excitation force. Since the reference signal into the amplifier is also outside the bandwidth of the amplifier, the current produced by the amplifier can't follow the reference signal. (See the frequency response of the amplifier in Figure 4.) The degradation of the current leads to a degradation of the velocity of the actuator; in particular, the current is no longer in phase with the reference signal. Since the velocity of the actuator follows the current, the velocity is no longer in phase with the external excitation force. This phase mismatch leads to a loss of transfer power. Therefore, the amplifier has lost the ability to control the flow of power out of the actuator when the system is operating outside the amplifier bandwidth.

## CONCLUSIONS

In this paper we have analyzed the power flow through the amplifier and actuator in a smart skin. Using an integrated model of the amplifier and actuator, the mechanical admittance of the amplifier and actuator as seen by an incoming acoustic wave is derived. It is shown that the mechanical impedance is shaped by the frequency response of the amplifier. It is also shown that this mechanical admittance depends on the acoustic feedback employed by the smart skin. By appropriate choice of the acoustic feedback controller, the power coupling between the actuators (acoustic piston) and the fluid can be increased. Moreover, the acoustic feedback can be used to match the mechanical admittance of the acoustic piston to the admittance of the fluid for optimal power coupling.

The internal power flow through the amplifier and actuator is also analyzed through simulation using a nonlinear model of the amplifier and actuator. It is shown that most of the electrical power in the amplifier is being converted into mechanical power in the actuator and then returned as electrical power to the power bus. Most of the electrical power is being cycled as charge flow in and out of the actuator (a capacitor). Hence, one of the main design requirements of an amplifier for electrostrictor and piezoelectric actuators is to manage this charge flow with minimal power dissipation.

The electrical power generated in the actuator due to the applied external force (the transfer power) is calculated. This power is transferred to the power bus by the amplifier when the acoustic control loop is properly designed and the amplifier is operated within its bandwidth. When the amplifier is operated outside its bandwidth, the transfer power is reduced and it is no longer unidirectional. There is a local cycling of power. This analysis highlights the importance of the frequency response of the amplifier in the power flow through the amplifier. Effective power flow occurs only when the frequency of the external force is within the bandwidth of the amplifier.

This analysis lends insight into the way that an actuator processes power. Because the various power signals are mismatched, this analysis suggests that the stroke/force characteristics of the actuator are mismatched.

## ACKNOWLEDGMENTS

The first author is supported in part by the Webber Teaching Fellowship. This research was supported in part by Virginia Power Technologies, Inc. under grant 121, and in part by Lockheed

Martin under grant SK30G4480. The prime contract is from DARPA under grant number N0014-95-C-0037. Dan Sable and Troy Schelling from Virginia Power Technologies, Inc. contributed to the design and fabrication of the switchmode amplifier.

## REFERENCES

Brennan, M. C. and A. R. McGowan. 1997. "Piezoelectric power requirements for active vibration control," *Proceedings of SPIE's 1997 North American Symposium on Smart Structures and Materials: Mathematics and Control in Smart Structures*, Vasundara V. Varadan and Jagdish Chandra; Ed., San Diego, CA, 3039:660-669.

Bridger, K. et al. 1996. "High-resolution medical ultrasound arrays using smart materials technology", *Proceeding of SPIE's 1996 North American Symposium on Smart Structures and Materials: Industrial and Commercial Applications of Smart Structures Technologies*, C. Robert Crowe; Ed., San Diego, CA, 2721:303-313.

Flint, E., C. Liang and C. A. Rogers. 1995. "Electromechanical analysis of piezoelectric stack active member power consumption," *Journal of Intelligent Material Systems and Structures*, 6(1):117-124.

Hagood, N. W., W. H. Chung, and A. von Flotow. 1990. "Modeling of Piezoelectric Actuator Dynamics for Active Structural Control," *Journal of Intelligent Material Systems and Structures*, 1(3):327-354.

Hom, C. L. and N. Shankar. 1994. "Fully coupled constitutive model for electrostrictive ceramic materials," *Journal of Intelligent Material Systems and Structures*, 5(6):795-801.

Kinsler, L. E., et al. 1982. *Fundamentals of Acoustics*, Third Edition, John Wiley & Sons, New York.

Liang, C., F. P. Sun and C. A. Rogers. 1994. "Coupled electro-mechanical analysis of adaptive material systems - determination of the actuator power consumption and system energy transfer," *Journal of Intelligent Material Systems and Structures*, 5(1):12-20.

Lindner, D. K., V. G. DeGiorgi, and S. H. McDermott. 1997. "Integrated Electronic/Material/Structural Modeling of a Smart Material," *Proceedings of the SPIE's 1997 North American Symposium on Smart Structures and Materials*, Marc E. Regelbrugge; Ed., San Diego, CA, pp. 3041:10-20.

Niezrecki, C. and H. H. Cudney. 1994. "Improving the power consumption characteristics of piezoelectric actuators," *Journal of Intelligent Material Systems and Structures*, 5(4):522-529.

Sable, D. M., R. B. Ridley, and B. H. Cho. 1990. "Comparison of performance of single-loop and current-injection-control for PWM converters which operate in both continuous and discontinuous modes of operation," *Proceedings of the IEEE Power Electronics Specialists Conference and Exposition*, San Antonio, TX, 74-79.

Zhou, S. and C. A. Rogers. 1995. "Power flow and consumption in piezoelectrically actuated structures," *AIAA Journal*, 33(7):1305-1311.

Zvonar, G. A. and D. K. Lindner. 1997a. "Nonlinear Electronic Control of an Electrostrictive Actuator," *Proceedings of SPIE's 1997 North American Symposium on Smart Structures and Materials: Industrial and Commercial Applications of Smart Structures Technologies*, Janet M. Sater; Ed., San Diego, CA, 3044:448-458.

Zvonar, G. A. and D. K. Lindner. 1997b. "Power Flow Analysis of Electrostrictive Actuators Driven by a PWM Amplifier," *Proceedings of the Adaptive Structures and Materials Systems Symposium*, D. Brei and J. Sirkis, Eds., 1997 ASME International Mechanical Engineering Congress and Exposition, Dallas, Texas, 54:155 - 162.

Zvonar, G. A. et al. 1996. "High-Frequency Switching Amplifiers For Electrostrictive Actuators", *Proceeding of SPIE's 1996 North American Symposium on Smart Structures and Materials: Industrial and Commercial Applications of Smart Structures Technologies*, C. Robert Crowe; Ed., San Diego, CA, 2721:465-475.

Zvonar, G. A., D. K. Lindner, and R. Goff. 1998. "Power Flow Through Amplifiers Controlling Electrostrictive Actuators," *Proceeding of SPIE's 1998 North American Symposium on Smart Structures and Materials: Industrial and Commercial Applications of Smart Structures Technologies*, Janet M. Sater; Ed., San Diego, CA, Vol. 3326.